Raquel Carvalho
Instituto Superior Técnico, University of Lisbon
Lisbon, Portugal (December 2020)
raquelsilvacarvalho@tecnico.ulisboa.pt

Numerical Analysis of Helical Piles Under Axial Loading

Influence of the number of helical plates, helical spacing and the conditions at the base

Abstract: The work here presented comprises the literature review about helical piles (HP), including a survey of the existing analytical methods to estimate the axial capacity. Having identified the existence of several analytical approaches, for two of the most used methods, the main differences were recognized and the results estimated from these were compared with those obtained from the axisymmetric numerical analyses performed by ABAQUS, a computer software suite for finite element analysis. In the absence of literature regarding numerical modelling of HP, simulation results were validated with compression responses of a single axially loaded pile. Based on this numerical validation, two more simulations were performed: i) a parametric study, to understand the effect of varying the number of helical plates and the helical plate spacing on the failure surfaces of vertically loaded axial piles, in both compression and tension, in cohesive soils; ii) a further analysis to study the behaviour of HP in compression, in a two-layered soil.

Through the parametric study, it was possible to identify a good agreement between the reported failure mechanisms, for the considered helical plate spacings, and the results of the performed analysis. Nevertheless, regarding the accuracy of the existing analytical approaches reviewed in this thesis, a new analytical formulation is proposed, based on the obtained numerical results.

Regarding the analysis on the two-layered soil, as no specific method was found in the literature, a generic approach was compared with the numerical analysis developed. Again, given its suitability, a new analytical formulation is also proposed.

Keywords: Helical piles; Pile design; Axial load; Failure mechanisms; Numerical modelling; Analytical methods.

1 Introduction

Helical piles are commonly used in other countries for over 180 years and, nowadays, there are more than 50 manufacturing companies on 4 of the 6 continents [1]. However, in Portugal there is no record that helical piles have ever been used in the civil construction sector. Since this type of foundation is an alternative to current indirect foundations, in a wide range of solutions, helical piles are considered an important tool in the geotechnical design.

Despite all the advantages associated with this type of foundation, there are still some knowledge gaps. In the available literature, it is common to find some highlights regarding the significant disparity between the theoretically predicted results and those measured in load tests. Thus, this issue may overturn the economic advantage of this solution since an efficient design is only achievable through load tests in multiple piles. Therefore, there is an urgent need to carry out further studies on this type of foundation, to find more accurate methods to estimate the pile capacity.

2 Literature review: design methods

There are two methods for predicting HP capacity, based on theoretical soil mechanics, namely, individual bearing and cylindrical shear.

2.1 Individual bearing method

The individual bearing method failure is explained by each helix behaving independently, since the spacing between helical plates is very large. A free body diagram showing an idealized distribution of the forces involved in this method is shown in Figure 1(a). Under compressive loading, the parameters affecting the bearing capacity will depend on the undisturbed soil bellow each helical plate, whereas under tension, the uplift capacity will depend on the disturbed soil above it. Adhesion stresses are assumed along the length of the shaft. Thus, the overall capacity of a HP, R, is the sum of the individual capacities of all the helical plates, $R_{h,i}$, along with the shaft resistance, R_f [1-3]:

$$R = \sum_{i}^{n} R_{h,i} + R_f \quad (1)$$

The shaft resistance is a function of its surface lateral area that depends on the length of the shaft, L. Skempton [1] showed that the bearing capacity factor, N_c, approaches a constant value of 9 for deep foundations. Therefore, it is usual to consider $N_c = 9$ and several authors follow this approach [1-4]. As cohesion of the soil can be taken as the undrained shear strength, S_u, in cohesive soils, the capacity of the HP by the individual bearing method is given by:

$$R = \sum_{i}^{n} 9S_u A_i + \alpha S_u L(\pi d) \quad (2)$$

Where A_i is the area of helical plate i, α is the adhesion factor between soil and the shaft and d is the diameter of the HP shaft.

2.2 Cylindrical shear method

The cylindrical shear method assumes that the entire volume of soil between helical plates is mobilized, acting as a semi-rigid body that develops a cylindrical shear surface.

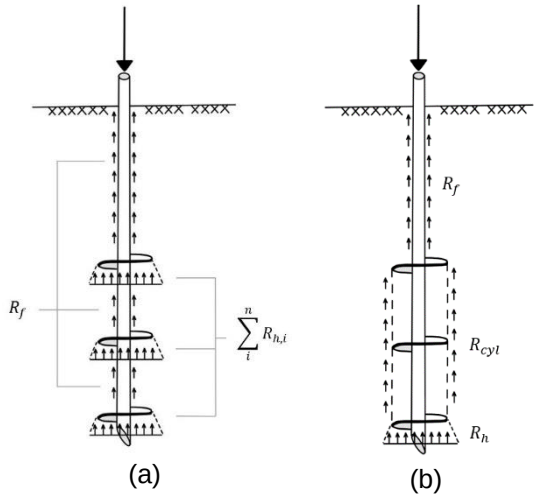

Figure 1: Forces involved on a HP under compression for (a) individual bearing method; (b) cylindrical shear method

This happens when the spacing between helical plates is small. A free body diagram showing the forces involved on the HP for cylindrical shear method is shown in Figure 1(b). Thus, the overall capacity of a HP based on this method is defined as a combination of shear along the cylinder, R_{cyl}, individual capacity of the bottom (for compressive loading) or the top helical plate (for HP under tension), R_h, and shear along the HP, R_f, being given by:

$$R = R_h + R_{cyl} + R_f \quad (3)$$

Nevertheless, in the cylindrical shear method, the surface lateral area of the helical shaft depends on its length above the top helix. Thus, taking $N_c = 9$ and $c = S_u$, it is possible to rewrite equation 3 as

$$R = 9S_u A_h + S_u(n-1)\, s\pi D + \alpha S_u H_T(\pi d) \quad (4)$$

Where A_h is the area of the bottom helix, for compressive loading, or the area of the top helix, for tensile loading, n is the number of helices, s is the spacing between helical plates, D is the diameter of the helical plates and H_T is the length of the helical pile shaft located above the top helix. All other parameters have been defined previously.

3 Numerical analysis: parametric study of helical piles in homogenous soil

3.1 Parametric study

The aim of the parametric study is to understand the effect of varying the number of helical plates, n, and the helical plate spacing, s, on the failure mechanisms of helical piles under compressive or tensile axial loads. Thus, keeping n constant, it is possible to ascertain the results as function of s/D, and the other way around. It was decided to study s/D modelling HP provided with 2 or 3 helical plates, varying the distance between pile top and bottom helical plates (L_c), since it is also intended to study the influence of n on the pile capacity.

In Figure 2 is showed a typical helical pile and all the dimensional parameters defined in the parametric study, where e_f is the pile shaft thickness, e_h is the thickness of helical plates and H_B is the distance between pile bottom and the bottom helical plate. All other parameters have been defined previously. As a helical pile is classified as deep if, at ultimate collapse, the observed failure mechanism is characterized by localised shear around the helical plates and is not affected by the location of the soil surface [5], the depth of the top helix (H_T) was defined to ensure a failure mode of this type.

The value of the considered helical plate spacing ratios, s/D, was based on the values pointed out by several authors as the ideal spacing of helical plates- where results from

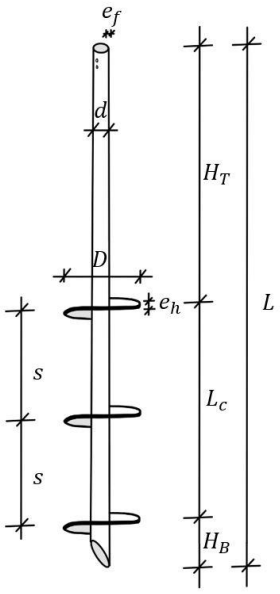

Figure 2: Dimensional parameters of a typical HP

individual bearing and cylindrical shear methods are equal.

In Table 1 is presented in detail all the dimensions of the helical piles analysed in the parametric study.

3.2 Analytical methods

Several authors focused on this topic and have established multiple analytical approaches to estimate the helical pile capacity using both individual bearing and cylindrical shear methods. Therefore, some of the existing analytical approaches in the literature were reviewed (Table 2). All the analytical formulations studied adopt $N_c = 9$ and the main differences are related to i) consider shaft resistance as a resisting force; ii) the value of the adhesion factor; iii) consider the overburden

Table 1: Dimensions of the helical piles analysed in the parametric study

n	d [mm]	e_f [mm]	D [mm]	e_h [mm]	H_B [mm]	L_c [mm]	H_T [mm]	L [mm]	s [mm]	s/D	Case name
2	89	5,5	254	12,7	10	254	3500	3764	254	1,0	H2SD1,0
						381		3891	381	1,5	H2SD1,5
						508		4018	508	2,0	H2SD2,0
						635		4145	635	2,5	H2SD2,5
						762		4272	762	3,0	H2SD3,0
						889		4399	889	3,5	H2SD3,5
3						508		4018	254	1,0	H3SD1,0
						762		4272	381	1,5	H3SD1,5
						1016		4526	508	2,0	H3SD2,0
						1270		4780	635	2,5	H3SD2,5
						1524		5034	762	3,0	H3SD3,0
						1778		5288	889	3,5	H3SD3,5

pressure above helices.

In Figure 3 the estimates for the pile capacity obtained by the different analytical approaches for the group of piles with two and three helical plates are presented. In both cases, the results vary over a considerably wide range: approximately 20 kN for group H2, and between 20 to 30 kN for group H3. In both sets, the approaches of H. A. Perko and R. W. Stephenson appear to be the most conservative. The Rao, Prasad and Shetty, Rao Prasad and Veeresh and Clemence's approaches present estimates that are closer to each other - these three approaches apply the cylindrical shear method. Stephenson's approach, using the cylindrical shear method, despises the shaft resistance and, therefore, demonstrates to be more conservative, as already mentioned.

Comparing the approaches that uses the individual bearing method, the estimates obtained according to Adams & Klym's approach stand out from the remaining for two main reasons: i) for small helical plate spacing ratios, the highest value for the pile capacity is determined by this approach; ii) for larger helical plate spacing ratios, the estimates are close to the results obtained by the cylindrical shear method. The first reason is because Adam & Klym consider the total length of the shaft to the shaft resistance, which added to the resistance of the various helices exceeds the pile capacity estimates according to the cylindrical shear method. The second point is motivated by the consequent increase of the estimates by the cylindrical shear method with the increase of the helical plate spacing ratio.

H. A. Perko's approach estimates the lowest pile capacity calculated using both methods. Thus, for the considered geometries, the cylindrical shear method proves to be

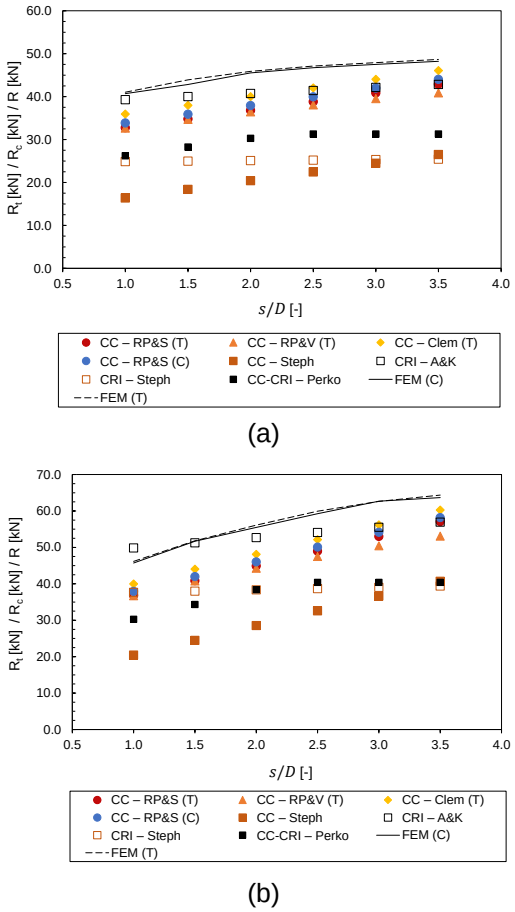

Figure 3: Pile capacity obtained through theoretical and numerical methods (a) H2; (b) H3

conditional for $s/D \in [1{,}0; 2{,}0]$, while the individual bearing method controls the pile capacity for $s/D \in [2{,}5; 3{,}5]$ - R is constant in this range for this reason.

For larger helical plate spacing ratios, in H3 set, the results from Perko's and Stephenson's are similar. Perko only consider the shaft resistance along the length of the shaft until the top helix, while Stephenson totally despises the adhesions stresses along the shaft in pile capacity calculations.

Table 2: Analytical approaches reviewed

Method	Direction of the force	Author(s)	Year	Label
Cylindrical shear method	Tension	Rao, Prasad & Shetty [4,6,7]	1991	CC – RP&S (T)
		Rao, Prasad & Veeresh [8]	1993	CC – RP&V (T)
		S. P. Clemence [9]	1985	CC – Clem (T)
	Compression	Rao, Prasad & Shetty [4,6,7]	1991	CC – RP&S (C)
	Compression/Tension	R. W. Stephenson [10]	2003	CC – Steph
Individual bearing method	Compression/Tension	Adams & Klym [7]	1972	CRI – A&K
		R. W. Stephenson [10]	2003	CRI – Steph
Both	Compression/Tension	H. A. Perko [1]	2009	CC-CRI – Perko

3.3 Numerical modelling

The displacement finite element software ABAQUS was used to perform all the numerical simulations. In the absence of literature regarding numerical modelling of HP, simulation results were validated with compression responses of a single axially loaded pile. The ABAQUS models consisted of a part divided in several partitions: the soil and its mesh refinement zones, and the helical pile. The soil was modelled as an elasto-perfectly plastic with failure described by the Drucker-Prager yield criterion. The elastic behaviour was defined by a Poisson's ration equal to 0.48, and a ratio of Young's modulus to shear strength of $E/S_u = 400$. The steel was modelled as an elastic material defined by a Poisson's ration equal to 0.30, and a Young's modulus of 210 GPa. The overall mesh dimensions were selected to ensure that the zones of plastic shearing and the observed displacement fields were contained within the model boundaries. A typical part for this problem, along with the applied displacement boundary conditions is shown in Figure 4. To determine the collapse load of the HP, a prescribed displacement was applied in the top of the pile [5].

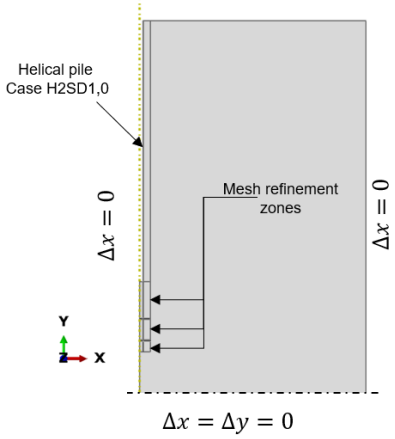

Figure 4: ABAQUS model and boundary conditions

Figure 5 shows the displacement field of the set of models run with 2 helices. It is possible to confirm the confirm the two failure mechanisms described in the literature. In Figure 5(a) and (b) the entire volume of soil between helical plates is mobilized and develops a cylindrical shear surface, while in Figure 5(e) and (f) each helix behaves independently as explained by the individual bearing method. The results of the analysis H2SD2,0 (C) and H2SD2,5 (C) seem to suggest a transition zone between both failure mechanisms, since the formed cylinder no longer displays the width of the helical plates and there is no clear individual response around the helices (Ficure 5(c) and (d)).

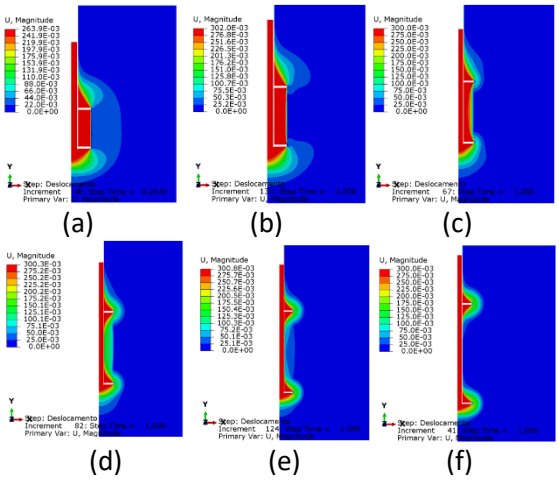

Figure 5: Contour displacements illustrating failure mechanisms (a) H2SD1,0 (C); (b) H2SD1,5 (C); (c)H2SD2,0 (C); (d) H2SD2,5 (C); (e) H2SD3,0 (C); (f) H2SD3,5 (C)

Figure 6 shows the displacement field of the set of models run with 3 helices. The behaviour is similar to the results observed previously: for small helical plate spacing ratios, the cylindrical shear surface is observed. However, comparing the models with the same helical plate spacing ratios in both sets of HP, the cylindrical shear surface seems to develop for higher s/D when $n = 3$. Thus, in set H3, the transition between the two failure mechanisms seems to occur in H3SD2,5(C) and H3SD3.0(C).

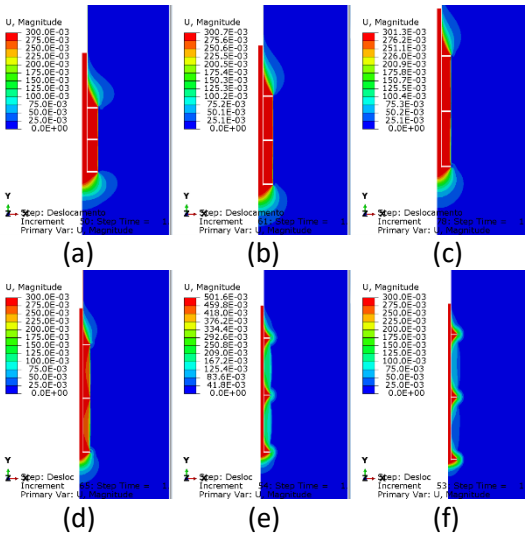

Figure 6: Contour displacements illustrating failure mechanisms (a) H3SD1,0 (C) (b) H3SD1,5 (C); (c)H2SD2,0 (C); (d) H3SD2,5 (C); (e) H3SD3,0 (C); (f) H3SD3,5 (C)

Figure 7 shows the load-displacement curves of the various analyses and it is possible to conclude that pile capacity increases with the increase of the helical plate spacing ratio, s/D. The results also seem to suggest that the foundation0s response is more fragile with the increase in s/D. The analyses performed on HP under tensile and compression loading also led to the conclusion that the bearing capacity is similar to the pull-out capacity, for deep helical piles.

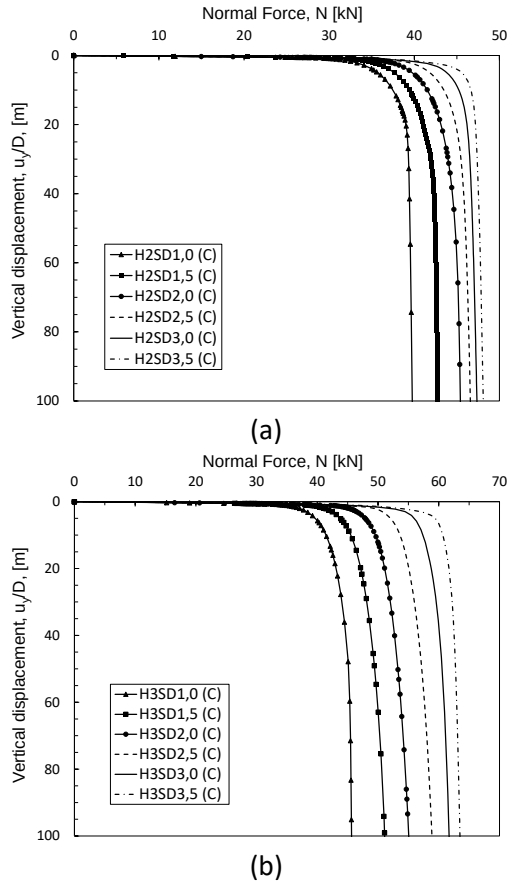

Figure 7: Load-displacement curves (a) H2(C); (b) H3(C)

3.4 Proposed analytical formulation

Given the significant differences obtained in the estimation of pile capacity (Figure 3), a new analytical formulation was developed. These differences are in line with what is highlighted by several authors in the literature, which emphasize the low suitability of these methods to estimate the pile capacity of helical piles.

Therefore, the proposed analytical formulation (PAF) recommends adopting a bearing capacity factor more adjusted to the specific behavior of this type of piles. Merifiel and Smith [5] had already stated this issue, concluding that the maximum total capacity of a helical plate cannot exceed the sum of the individual helical plate capacities. Also considering what Perko [1] proposed, the pile capacity, according to the PAF, results from the least value obtained both methods.

It was concluded that, when helical plates act independently of each other ($s/D = \{3{,}0; 3{,}5\}$), the bearing capacity factor presented by Rowe seems to fit very well the results obtained, both numerically and in the shape of the failure surface (Figure 8). Thus, the PAF adopts the same bearing capacity factor to apply the individual bearing method.

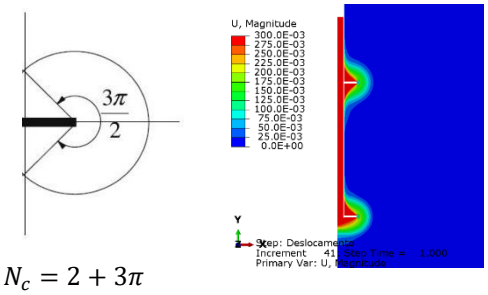

$N_c = 2 + 3\pi$

(a) (b)

Figure 8: (a) Upper bound mechanism for deep failure mode by Rowe (1978, adapted from [5]); (b) Contour displacements of H2SD3,5 (C)

Based on the results from the performed numerical analyses, the PAF also assumes adhesion stresses along the entire length of shaft. Therefore, the pile capacity of a HP using the individual bearing method is given by:

$$R = \underbrace{\sum_{i}^{n} (2 + 3\pi) S_u A_i}_{R_h} + \underbrace{\alpha S_u L(\pi d)}_{R_f} \quad (5)$$

When the spacing between helices is reduced, the shape of the failure surface developed next to the top helix is similar to that observed next to the bottom helix. Thus, and because the developed stresses near the top and bottom helices resembles that of a simple pile with diameter D, the PAF suggest the adoption of $N_c = 9$. The pile capacity of a HP using the cylindrical shear method, according to the PAF, is given by:

$$R = \underbrace{(9 S_u A_h) \times 2}_{R_h} + \underbrace{S_u (n-1)\, s\pi D}_{R_{cil}} + \underbrace{\alpha S_u H_T (\pi d)}_{R_f} \quad (6)$$

All the parameters have been defined previously.

Figure 9 shows the results for the pile capacity obtained according to the PAF and through numerical analysis. For set H2, the individual bearing method controls the pile capacity for $s/D > 1{,}5$, whereas for set H3 the estimated pile capacity is limited by this method when $s/D > 3{,}0$. Comparing the analytical results with those obtained by ABAQUS, it is possible to verify a very good agreement between the pile capacity estimated according to the PAF and that obtained by the FEM to both tensile and compressive loading. The obtained relative error between these results is less than 5% for the helical plate spacing ratios considered.

Since the mechanisms by which helical piles develop resistance to the load are described in a manner consistent with basic principles of soil mechanics, pile capacity increase with the increase of helical plate spacing ratio. When helices act together, this increase it is a function of the diameter of helical plates, D. On the other hand, when helical plates act independently of each other, the increase of the pile capacity becomes a function of the diameter of the helical pile shaft, d.

It is also possible to verify in Figure 9 that helical piles with two helices follow the behaviour described by the cylindrical shear method for small s/D, whereas for larger helical plate spacing ratios, HP follow the behaviour described by the individual bearing method. For $n = 3$, the individual bearing method only seems to be conditioning the behaviour of the helical plates for $s/D > 3{,}0$. Thus, for helical plate spacing ratios lower than this value, the helical plates do not seem to present an individual response.

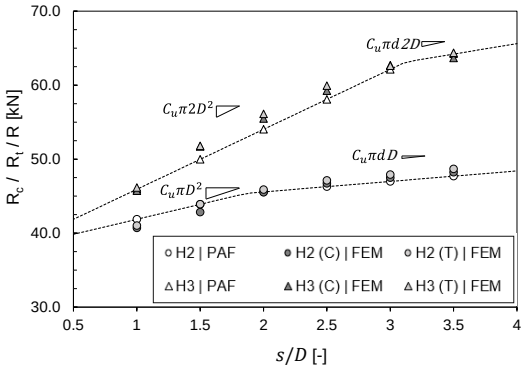

Figure 9: Pile capacity obtained according to the PAF and through numerical analysis

Therefore, the PAF suggests the following behaviour for helical piles:

- $s/D < 2{,}0$ – failure mechanism described by the cylindrical shear method;
- $2{,}0 < s/D < 3{,}5$ – transition zone between the two methods;
- $s/D > 3{,}5$ – failure mechanism described by the individual bearing method.

This should be taking into the account in the design of helical plate, having in mind that the behaviour of this foundations depends on the helical plate spacing ratios.

4 Numerical analysis: behaviour of helical piles in two-layered soil

In fact, the geotechnical project is not always confronted with the scenario proposed in the previous chapter, in which the surface layer, of low resistance, extends several meters deep. Instead, is more common that this layer is based on a more resistant substratum. Thus, it is intended to study the influence of the conditions at the base of the HP. It was chosen to model only the helical piles with smaller and greater helical plate spacing ratios of the set of piles with two helices, namely H2SD1,0 and H2SD3,5. However, to understand the impact of the top helix in the bearing capacity, the same piles were modelled without this helix. Theses analyses were called H1SD1,0 and H1SD3,5. To differentiate the results obtained in the previous chapter from those obtained in this one, from now on, it will be added to the case names the following acronyms: 1L, for analyses performed in homogenous scenario, and 2L, for analyses performed in a two-layered soil.

4.1 Analytical methods

As no specific method was found in the existing literature to estimate the pile capacity in a two-layered soil, a generic approach was compared with the numerical analysis developed. It was chosen to compare the H. A. Perko's approach, presented in Perko [1], one of the most complete books on the subject. Therefore, in Table 3 is presented the bearing capacity estimated for the different cases. There is no difference regarding the calculation method in

Table 3: Bearing capacity estimated according to Perko [1]

Case name	R_h [kN]	R_{cil} [kN]	R_f [kN]	$R_{h,t}$ [kN]	$R_{h,b}$ [kN]	R_c [kN]
H1SD1,0 | 2L	91,2	-	14,0	-	91,2	105,2
H1SD3,5 | 2L	91,2	-	16,4	-	91,2	107,6
H2SD1,0 | 2L	91,2	4,1	13,0	9,1	91,2	108,3
H2SD3,5 | 2L	91,2	14,2	13,0	9,1	91,2	113,4

cases H1SD1,0 and H1SD3,5, since the HP are modelled with just one helix. In set H2, the cylindrical shear method controls the bearing capacity when $s/D = 1{,}0$, whereas the individual bearing method is conditional when $s/D = 3{,}5$. These results are similar to those estimated in homogenous soil.

Unlike the homogenous scenario, Perko's approach overestimates the bearing capacity of HP in two-layered soils. Figure 10 shows the diagrams of the applied normal force along the shaft's depth, estimated according to Perko [1] and obtained through numerical analyses. Although the difference in the overall bearing capacity varies between 11,6% and 16,6%, the greatest gap concerns the calculation in the helical plates' capacity. The bottom helix's capacity is drastically overestimated, unlike the top helix.

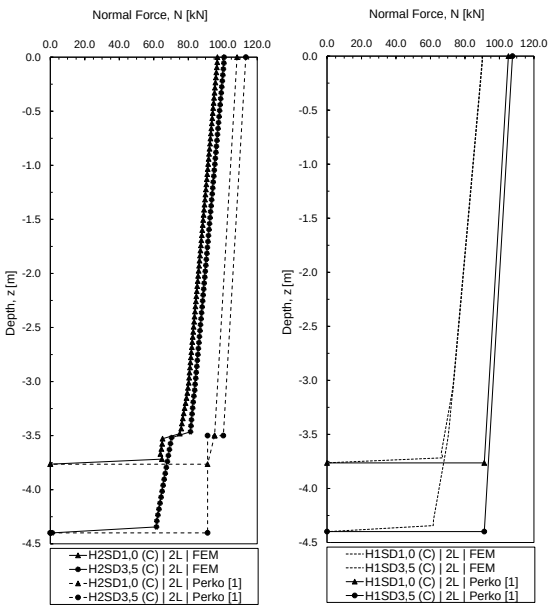

Figure 10: Normal force VS Depth estimated according to Perko [1] and obtained through numerical analysis

4.2 Numerical modelling

Again, the displacement finite element software ABAQUS was used to perform the numerical simulations, which follow what was presented in section 3.3. To simulate the more resistant substratum, another material was created, similar to the soil previously defined. Thus, the difference between the two layers of soil is the ratio of Young's modulus to shear strength. The bottom layer is defined by a $E/S_u = 1000$.

Figure 11 shows the load-displacement curves of the analyses in homogenous and two-layered soil. The overall bearing capacity is achieved for displacements approximately equal to 10% of the diameter, D. The presence of a more resistant layer at the base increases substantially the bearing capacity of the HP. In the results obtained, the bearing capacity of a HP in a two-layered soil increased by more than twice as much as in homogeneous soil.

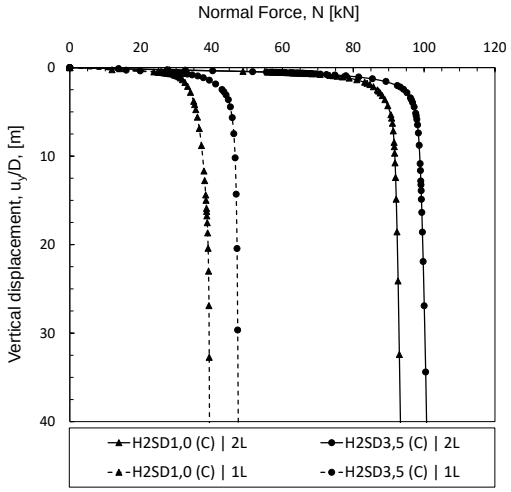

Figure 11: Load-displacement curves

Figure 12 shows the diagrams of the applied normal force along the shaft's depth. The difference in the bottom helix's bearing capacity is evident, which is proportional to S_u, as would be expected. Thus, it is possible to confirm that the observed increase is a consequence of the developed resistance to the load by the bottom helix. The same figure seems to suggest that the difference in the bearing capacity of models H2SD1,0 (C) | 2L and H2SD3,5 (C) | 2L is due

to the length of the pile shaft between both helices. It should also be noted that the increase in the bearing capacity between $s/D = 1{,}0$ and $s/D = 3{,}5{,}5$ in two-layered soil is slightly lower, given the resistance mobilized by the bottom helix.

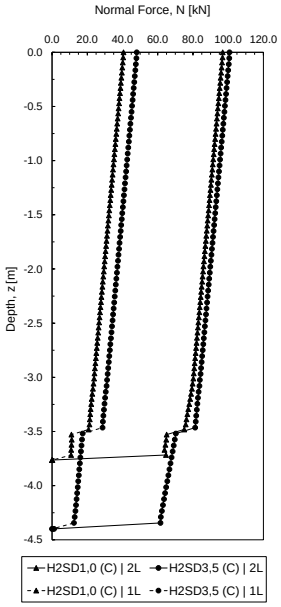

Figure 12: Normal force VS Depth

4.3 Proposed analytical formulation

Given the significant differences obtained in the estimation of bearing capacity and the suitability of the analytical approach, a new analytical formulation is proposed.

Analysing manly the resistance mobilized by the bottom helix, it is understood that the bearing capacity factor applied, $N_c = 9$, is inadequate. The numerical analysis performed suggests a lower value. Therefore, in Figure 13 the failure surfaces of H2SD1,0 (C) and H2SD3,5 (C) in homogenous and two-layered soil are compared. It is possible to confirm that the size of the failure surface is smaller in the second case. Since the results do not present significant differences in the behaviour of the top helix, the PAF discussed earlier in section 3.4 was adopted in this helix.

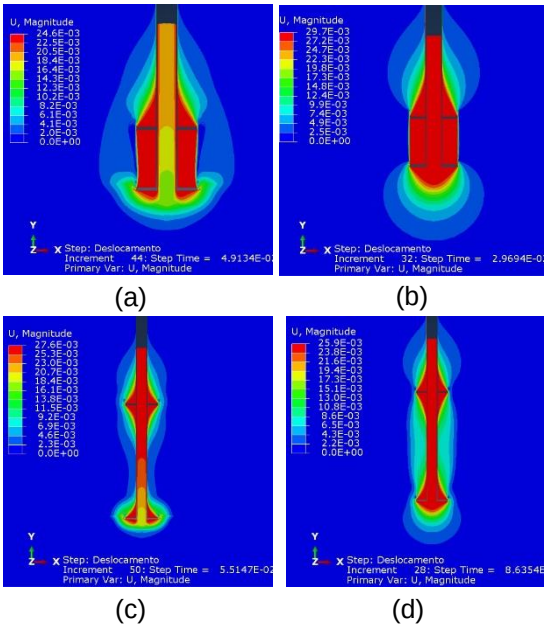

Figure 13: Contour displacements (a) H2SD1,0 | 2L; (b) H2SD1,0 | 1L; (c) H2SD3,5 | 2L; (d) H2SD3,5 | 1L

For the bottom helix, considering the suggestion to adopt a lower value for N_c, and taking into account the shape of the failure surface developed next to the base of the HP, it was taken $N_c = 2\pi$. Thus, in Table 4 the results obtained are presented, as well as the relative error between the bearing capacity estimated according to the PAF and that obtained by the FEM. Figure 14 also compares the diagrams of the applied normal force along the shaft's depth, estimated according to the PAF and obtained through numerical analyses. It is possible to verify a very good agreement between the results estimated according to the PAF and that obtained by the FEM. The maximum relative error obtained between these results was 1%.

However, another reason for the inadequacy of applying the same bearing capacity factor in both geotechnical scenarios may be related to the difference in layers' undrained shear strength. In order to access this explanation, new numerical analyses were performed, varying the values of layers' S_u.

Table 4: Bearing capacity estimated according to PAF and obtained through numerical analysis

Case name	PAF					FEM	Relative error [%]
	R_f [kN]	$R_{h,t}$ [kN]	R_{cil} [kN]	$R_{h,b}$ [kN]	R_c [kN]	R_c [kN]	
H1SD1,0 | 2L	21,0	-	-	63,7	84,7	90,2	6,1
H1SD3,5 | 2L	24,5	-	-	63,7	88,3	94,0	6,1
H2SD1,0 | 2L	19,6	9,1	4,1	63,7	96,4	97,1	0,7
H2SD3,5 | 2L	24,5	11,6		63,7	99,8	100,8	1,0

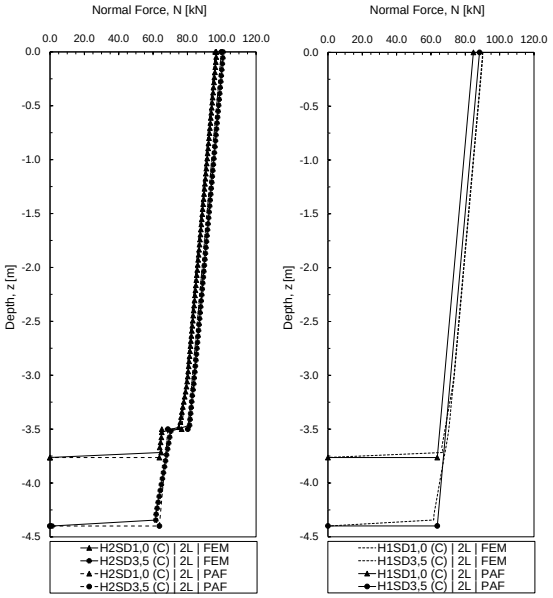

Figure 14: Normal force VS Depth estimated according to the PAF and obtained through numerical analysis

Thus, a new variable k is introduce:

$$k = \frac{S_{u,b}}{S_{u,t}} \tag{7}$$

Where k is the ratio of undrained shear strength of the top layer, $S_{u,t}$, to the undrained shear strength of the bottom layer, $S_{u,b}$.

In the analyses already presented, k is equal to 1 in the models run in homogenous soil, and equal to 10 in the models run in two-layered soil, with $S_{u,b} = 200\ kPa$. To be able to understand the evolution of N_c and confirm this hypothesis, four more numerical analyses were performed with $k = \{2; 5; 20; 60\}$. The results are presented in Figure 15.

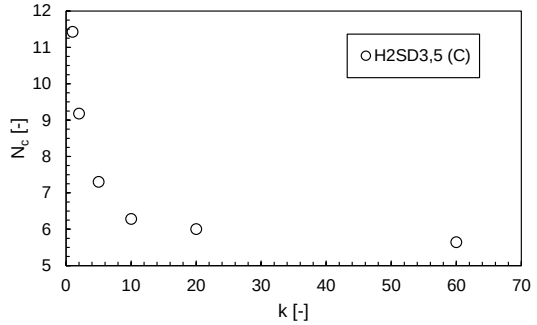

Figure 15: Bearing capacity factor VS k

With the increase of N_c, k tends to stabilize. It is reminded that the exact solution for vertically centered loading (isolated footings) in undrained conditions takes $N_c = 2 + \pi$ [11]. Therefore, it is expected that, the lower the value of $C_{u,t}$, N_c tent for this solution. On the other hand, if soil is homogeneous, the analyses seem to indicate $N_c = 2 + 3\pi$, which agrees with the discussed in the previous chapter.

Thus, the PAF suggest the adoption of a bearing capacity factor in the range expressed in equation 8, according to the value of the variable k.

$$2 + \pi < N_c \leq 2 + 3\pi \tag{8}$$

5 Conclusions

The numerical analysis developed allowed to fulfil the proposed objectives, recognizing the effectiveness of computational simulation to study this topic. It was possible to identify the two types of failure surfaces described in the existing literature and a good agreement was found between the reported failure mechanisms, for the considered helical plate spacings, and the results of the performed analysis. The pile capacity increases with the increase of the helical plate spacing ratio, s/D, as with the increase in the number of helices. The analytical approaches reviewed proved inadequate to estimate the pile capacity of HP, demonstrating to be conservative. It was found a great disparity between the pile capacity estimated according to the analytical approaches and that obtained by the numerical analysis. The presence of a more resistant layer has shown to significantly increase the bearing capacity of HP and modify the failure surfaces. Therefore, the existing analytical formulations to estimate pile capacity in homogeneous soil are inadequate. Bearing capacity factors must be adjusted to reflect the behaviour of helical piles in homogenous and two-layered soils. The two PAF show a good agreement with the results obtained in the numerical analysis performed. The PAF were validated for cohesive soils in undrained conditions.

References

[1] Perko, H. A. (2009). Helical piles: A practical guide to design and installation. John Wiley & Sons, Inc., Hoboken, New Jersey, EUA, 512 p, ISBN 978-0-470-40479-9.

[2] Mohajerani, A., Bosnjak, D. e Bromwich, D. (2015). Analysis and design methods of screw piles: A review. *Soils and Foundations*, 2016, 14 p. doi: 10.1016/ j.sandf.2016.01.009

[3] Lutenegger, A. J. (2009). Cylindrical shear or plate bearing? – Uplift behaviour of multi-helix screw anchors in clay. Proceedings of the *2009 International Foundation Congress and* Equipment, 456-463. doi: 10.1061/41021(335)57

[4] Rao, S. N., Prasad, Y. V. S. N. & Shetty, M. D. (1991). The behaviour of model screw piles in cohesive soils. *Soils and Foundations*, *31*(2), 35-50. doi:10.3208/sandf1972.31.2_35

[5] Merifield, R. S. & Smith, C.C. (2010). The ultimate capacity of multi-plate strip anchors in undrained clay. *Computers and Geotechnics, 37*, 504-514. doi: 10.1016/j.compgeo.2010.02.004

[6] Meyerhof, G. G., & Adams, J. I. (1968). The ultimate uplift capacity of foundations. *Canadian Geotechnical Journal,* Volume 5, n. º 4, 225-244. doi: 10.1139/t68-024

[7] Adams, J. I. e Klym, T. W. (1972). A Study of Anchorages for Transmission Tower Foundations. *Canadian Geotechnical Journal*, *9*(1), 89-104. doi:10.1139/t72-007

[8] Silva, B. C. (2014). Estimativa da capacidade de carga à tração de estacas helicoidais com base no ensaio SPT. Master's thesis in Geotechnics. Escola de Engenharia de São Carlos, Universidade de São Paulo. *(in Portuguese)*

[9] Stephenson, R. W. (1997). Helical foundations and tie backs: State of the art. Civil engineering department, University of Missouri-Rolla, julho 1997, 34 p.

[10] Stephenson, R. W. (2003). Design and installation of torque anchors for tiebacks and foundations. Master's thesis in Civil Engineering, Missouri University of Science and Technology.

[11] Guerra, N. (2012). Análise de estruturas geotécnicas. *Handouts of Theoretical Classes of Analysis of Geotechnical Structures course*, Instituto Superior Técnico, Universidade de Lisboa, 176 p. *(in Portuguese)*